Research Article   **Open Access**

Evaluation of Shadow Reconstruction Algorithm for Very High Resolution Satellite Imagery

Panchal Anjali Jayant [1,2], Rizvi Imdad A.[2] and Kadam M.M.[2]

[1]Department of Electronics and Telecommunication Engineering, Konkan Gyanpeeth College of Engineering, Karjat, Maharashtra, India
[2]Department of Electronics and Telecommunication Engineering, Terna Engineering College, Navi Mumbai, Maharashtra, India

Abstract The Very High Resolution images have opened a new era for remote sensing applications such as object detection, classification, object mapping and change detection. However, the effects of shadow in these images are remarkable. The objective of this paper is to propose algorithm for shadow reconstruction. The primer stage, shadow detection and classification are carried out which separates shadow from rest of environment. For doing reconstruction the preprocessing is done by morphological operations which extract image components such as region and shape. It is followed by border creation and finally the reconstructed of an original image is accomplished border interpolation. The reconstruction accuracy is calculated by using Kappa Coefficient. Here Experimental results are obtained on three VHR images representing different shadow conditions. The performance analysis is carried out which shows better sensitivity and specificity.
Keywords *Cast Shadow; Self-Shadow; Shadow Detection; Sensitivity; Specificity; VHR Satellite Images*

1. Introduction

The resolution of VHR image distinguishes very well defined features from small objects like building structures, trees, vehicles and roofs (Rizvi and Buddhiraju, 2011, 2012). But high spatial resolution causes some problems like presence of shadows particularly in urban areas where there are larger changes in surface elevation due to the presence of buildings, bridges, towers and longer shadows. (Lorenzi, Melgani and Mercier, 2012). However the analysis of these images also requires new digital image processing techniques to deal with challenges such as the problem of shadows (Jindong and Marvin, 2012).

In high resolution imagery presence of shadow leads to the reduction or total loss of spectroradiometric information which carry problems in the interpretation of land cover and the evaluation of ground condition depend (Susaki, 2012). To estimate the effects of shadow reconstruction, both pixel-based and object-oriented methods were used (Jindong and Marvin, 2013).

An invariant color space based non-linear transformation was projected, while histogram thresholding was performed to differentiate shadows from non-shadow areas in QuickBird and IKONOS images (Salvador et al., 2001), radiance ratio with digital numbers (Liu and Yamazaki, 2010) and with three dimensional models (Tsai and V.J.D, 2006; Chung et al., 2009). Additionally if the a priori knowledge of the sensor, the illumination, and the 3-D geometry of the scene are available, three-dimensional models have been developed (Scott and Narayanan, 2012).

The several radiometric restoration methods were compared to get rid of shadow areas in the original satellite imagery, (Sarabandi, 2004), with gamma correction, linear correlation correction (Chen, 2007) and histogram matching (Tsai and V.J.D, 2006). To swap shadow pixels in one image with non-shadow pixels of the same area from another image, multisource data fusion has also been used (Yuan, 2008). The shadow areas were easily extracted from the Quick Bird imagery by using the segmentation of a panchromatic image and a calculated radiance ratio between the shaded and sunlit areas (Liu and Yamazaki, 2012). Similarly to prepare an initial shadow mask, thresholding is adopted and then for shadow detection the noise and wrong shadow regions are isolated by the morphological phases (Song et al., 2013) and then reconstruction is carried out by linear correlation method.

The classification is also better approach for shadow reconstruction, considering most spectroradiometric restoration algorithms were not designed to optimize classification performance, a support vector machine approach (Buddhiraju and Rizvi, 2010) was used to classify shadows for shadow pixels in satellite imagery (Panchal et al., 2014).

Similarly the object-oriented methods produces better classifications because of its capacity of subdividing images into individual homogeneous regions (i.e., image objects) at scales that are appropriate to the inherent landscape (Rizvi and Buddhiraju, 2010) and establishing the context information and topological network of these image objects for accurate classification (Benz et al., 2004).

2. Proposed Method

In this case, the more interest is given in the land cover that casts the shadows (e.g., buildings and trees) than the land cover shaded by shadows (e.g., grass and impervious surfaces). In this work three satellite images are used which has impervious shadow structure. Most of the shadow structure is almost in rectangular shape as they cast on building, aircraft etc. The flowchart with principal steps of proposed system is shown in Figure 1. This is the extended work of (Panchal et al., 2015) in which shadow detection is already explained in detail. The brief review of shadow detection is explained further.
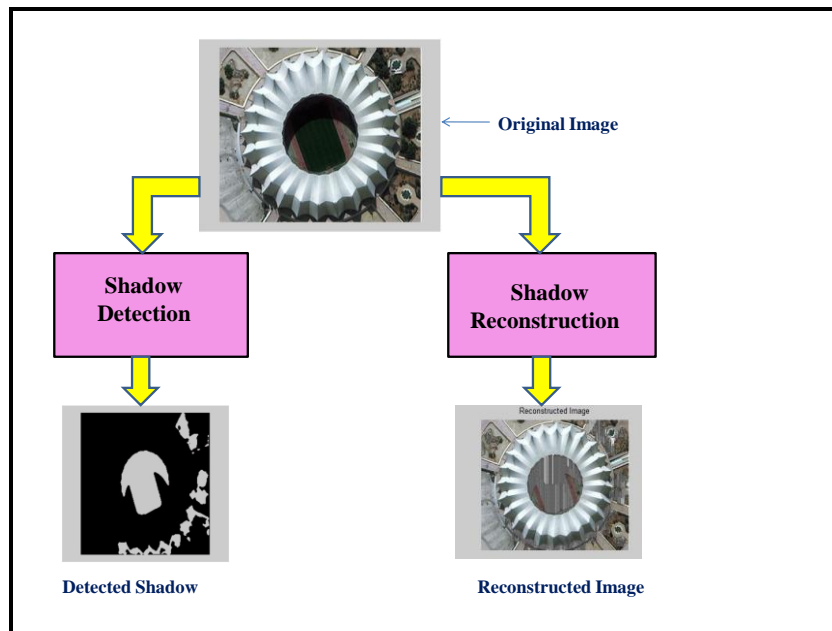
Figure 1: Flowchart of Proposed System

2.1. Shadow Detection Approach

In this paper, spectral values of satellite images are taken into consideration. To perform shadow detection the basic processing are done by following stages.

2.1.1. Thresholding

Threshold value is calculated from the same satellite images. Thresholding is simply the method of converting an image to binary format by setting all pixels whose values are greater than some threshold level to "high" and the remaining pixels to "low". It represents binary mask of a satellite image.

2.1.2. Morphological Filtering

The morphological operators are required in order to separate isolated shadow pixels in a non-shadow area and also isolated non-shadow pixels in a shadow area. Then the operations of erosion, dilation and morphological operation are performed. Erosion finds the correct points of shadow which are placed in neighborhood. The points which are found by erosion are connected by dilation.

2.1.3. Border Creation

The border is to be defined which shows transition in between the shadow and non-shadow areas. Otherwise it can raise problems such as boundary ambiguity, color inconstancy, etc. Therefore canny edge detection algorithm is used, so bordered image is found.

2.2. Shadow Reconstruction Approach

Here morphological operations are used for extracting image components such as region and shape. The structuring elements adopted to perform morphological opening operation and morphological closing operations are shown in Figure 2.

1	1	1	1	1
1	1	1	1	1
1	1	1	1	1
1	1	1	1	1
1	1	1	1	1

Figure 2: Structuring element for Opening operation and Closing operation

The opening operation smoothes the contour of an image whereas closing fuse the narrow breaks, eliminates small holes and fill gaps in contour. The output of these operations is post processed mask of an image. After this process again structuring element is applied of 10×10 matrix to have dilation of an image.

In this case, for doing reconstruction the simple step is carried out i.e. as we know the shadow is also surrounded by non-shadow region. It means if we calculate average value of non-shadow region in the neighborhood and then assign into shadow region, it will be seen as an image without shadow.

To do so, border $h[x, y]$ is created by subtracting dilated image with closing operation of an image and final mask is created with border.

$$h[x, y] = \partial[x, y] - Eclosebw[x, y]$$

(1)

The connected components of shadow region are searched out and assigned the pixel value to shadow region. In this case shadow values and non-shadow values are taken into consideration. The shadow values are selected and these intensity values should be replaced with non-shadow. For this purpose, nearest location of non-shadow value is calculated by considering the region of shadow pixel value added with 50 and shadow pixel value subtracted with 50. Within the same region, minimum value of non-shadow pixel is calculated and it replaces the shadow pixel. If minimum value is not identified then shadow pixel is replaced by nearby non shadow pixel within the region.
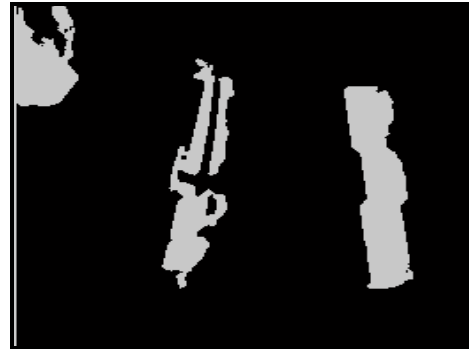
3. Results and Discussions

To evaluate the results of proposed method, three images were used. They differ from the properties (distribution and size) of the shadows which depend on the kinds of shaded land covers and the acquisition time. The aircraft image is of 634×403 dimensions with 69 dpi resolution as shown in Figure 3(a). The circular image is of 260×210 dimensions with 300 dpi resolution as shown in Figure 4(a). The road image is of 738×533 dimensions with 96 dpi resolution as in Figure 5(a).

3.1. Shadow Detection Output

As described in the previous section, the first task of the proposed methodology is to generate a mask image useful to localize the shadow, the non-shadow, and the border areas. Therefore to capture shadow, thresholding is carried out which create binary mask of an image. Similarly shadow detection outputs are shown in Figures 3(b), 4(b) and 5(b).

(a) Aircraft Image

(b) Detected Shadow

Figure 3: *(a) Aircraft Image (b) Detected Shadow*

(a) Circular Image

(b) Detected Shadow

Figure 4: *(a) Circular Image (b) Detected Shadow*

(a) Road Image

(b) Detected Shadow

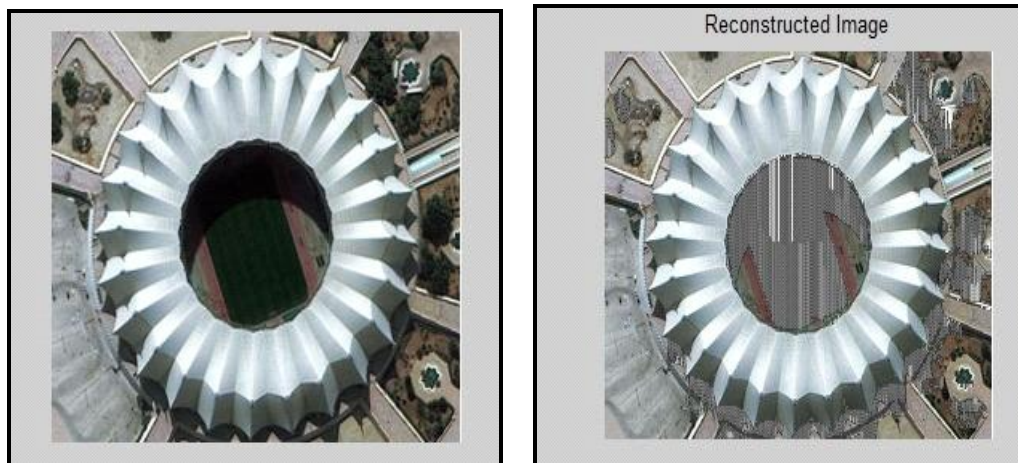**Figure 5:** *(a) Road Image (b) Detected Shadow*

3.2. Shadow Reconstruction Output

The shadow reconstruction output is shown with original images. The first image shows shadow structures in rectangular manner, therefore they are more properly reconstructed. But second image and third image, the dark vegetation areas are mistakenly represented as shadow area, so these

portions of an image is also reconstructed with shadow part. The figures are shown in 6(a), 6(b) and 6(c).

(a) Aircraft Image

(b) Circular Image

(c) Road Image

Figure 6: *Image Reconstruction output (a) Aircraft image (b) Circular image (c) Road image*

The reconstruction output's accuracy is also calculated in following manner i.e. by neural network. The User's Accuracy and producer's accuracy are observed weak. But Kappa Coefficient and Classification accuracy i.e. overall accuracy are observed in better manner.

Table 1: Classification Evaluated for Image Reconstruction

	User's Accuracy	Producer's Accuracy	Kappa Coefficient	Classification Accuracy
Aircraft Image	30	42.5	0.496	72.5
Circular Image	31	33	0.734	85
Road Image	25.8	40.8	0.493	74.5

4. Performance Analysis

To evaluate the performance of the given method, the following procedure is used. The classified output is compared with ground truth information to validate the results. The assumption is made that shadow pixels are of white as foreground and non-shadow pixels are black pixels as background in the ground truth. The following terms are used for doing analysis.

True positive (TP): pixels correctly classified as foreground
False positive (FP): pixels falsely classified as foreground
True negative (TN): pixels correctly detected as background
False negative (FN): pixels falsely detected as background

These metrics are then used to calculate sensitivity, specificity and accuracy as:

Sensitivity: The sensitivity of the method is proportion of positive pixels correctly predicted (i.e. the probability that a pixel belonging to shadow is correctly identified). This is calculated as TP/ (TP+FN).

Specificity: The specificity of the method is proportion of negative pixels correctly predicted (i.e. the probability that a pixel belonging to non-shadow is correctly identified). This is calculated as TN/ (TN+FP). Thus models with high sensitivity can correctly predict positive pixels (pixels belonging to the category of interest) and models with high specificity can correctly predict negative pixels (pixels not belonging to the category of interest). High sensitivity is usually associated with poor specificity, which manifests as an overestimate of area in the category of interest.

Accuracy: Accuracy is biased estimates that depend on the proportion of pixels actually belonging to each class. It is (TP+TN)/ (TP+FP+TN+FN).

Table 2: Performance Parameters Evaluation

	TP	FP	TN	FN
Aircraft Image	7435	1049	55618	1434
Circular Image	3048	9085	53384	19
Road Image	2236	3079	53781	6442

Table 3: *Performance Accuracy Evaluation*

	Sensitivity	Specificity	Accuracy
Aircraft Image	96.21	83.83	98.15
Circular Image	86.10	99.38	85.46
Road Image	85.47	25.77	94.58

The aircraft image is evaluated with correct shadow pixels classified as 3048, correct non shadow pixels 19. The non-shadow pixels 20995 are classified as shadow and 37525 shadow pixels are classified as non-shadow. Therefore sensitivity says that the correctly shadow pixels identified are 86.10%. Similarly specificity observed that the correctly non shadow pixels identified are 99.38% and accuracy 85.46%. Note that first image have larger shadow structure, therefore the result is good.

For the circular image is evaluated with correct shadow pixels classified as 7435, correct non shadow pixels 1434. The non-shadow pixels 1049 are classified as shadow and 55618 shadow pixels are classified as non-shadow. For this case image with sensitivity 96.21%, specificity 83.83%, 98.15% accuracy is observed.

The road image is evaluated with correct shadow pixels classified as 2236, correct non shadow pixels 6442. The non-shadow pixels 3079 are classified as shadow and 53781 shadow pixels are classified as non-shadow. Therefore sensitivity says that the correctly shadow pixels identified are 85.47%. Similarly specificity observed that the correctly non shadow pixels identified are 25.77% and accuracy 94.58%.

5. Conclusion

From obtained results, following points can be considered,

- The proposed method works well for grayscale images where shadows are in rectangular shapes. Therefore this method can be used for urban areas.
- The shadow reconstruction output is calculated by using neural network. It is observed that the Kappa Coefficient values for three images are greater than 50% and Classification Accuracy for three images gave above 70%.
- An optimum classification model would be one with the highest possible value of both sensitivity and specificity. From performance analysis, the classification accuracy, sensitivity, specificity are observed greater than 80%.

References

Benz, U.C., Hofmann, P., Willhauck, G., Lingenfelder, L. and Heynen, M. *Multi-Resolution, Object-Oriented Fuzzy Analysis of Remote Sensing Data for GIS-Ready Information.* ISPRS Journal of Photogrammetry Remote Sens. 2004. 58; 239-258.

Buddhiraju, K.M. and Rizvi, I.A., 2010: *Comparison of CBF, ANN and SVM Classifiers for Object-Based Classification of High Resolution Satellite Images.* Proc. IGARSS. 40-43.

Chung, Liang Kuo, Lin Yi-Ru, and Huang Yong-Huai. *Efficient Shadow Detection of Color Aerial Images Based on Successive Thresholding Scheme.* IEEE Transaction on Geosciences and Remote Sensing. 2009. 47 (2).

Chen, Y., Wen, D., Jing, L. and Shi, P. *Shadow Information Recovery in Urban Areas from Very High Resolution Satellite Imagery.* International Journal of Remote Sensing. 2007. 28; 3249-3254.

Jindong Wu and Marvin E. Bauer. *Evaluating the Effects of Shadow Detection on QuickBird Image Classification and Spectroradiometric Restoration.* Journal of Remote Sensing. 2013. 5; 4450-4469.

Lorenzi Luca and Melgani Farid, and Mercier Grégoire. *A Complete Processing Chain for Shadow Detection and Reconstruction in VHR Images.* IEEE Transaction on Geosciences and Remote Sensing. 2012. 50 (9).

Liu Wen and Yamazaki Fumio. *Shadow Extraction and Correction from Quick Bird Images.* IEEE J. Sel. Top. Appl. Earth Obs. Remote Sens. 2010. 978-1-4244-9566 5/10.

Liu, W., and Yamazaki, F. *Object-Based Shadow Extraction and Correction of High Resolution Optical Satellite Images.* IEEE J. Sel. Top. Appl. Earth Obs. Remote Sens. 2012. 5; 1296-1302.

Panchal, A.J., Rizvi, I.A. and Kadam, M.M., 2014: *Shadow Detection of Very High Resolution Satellite Images Using Support Vector Machine.* ISPRS TC VIII Mid-Term Symposium 2014.

Panchal, A.J., Rizvi, I.A. and Kadam, M.M. *Proposed Algorithm for Shadow Identification and Classification in VHR Satellite Imagery.* Journal of Remote Sensing & GIS. 2015. 6 (3) 2015.

Rizvi, I.A. and Buddhiraju, K.M. *Object-Based Image Analysis of High Resolution Satellite Images using Modified Cloud Basis Function Neural Network and Probabilistic Relaxation Labeling Process.* IEEE Transaction on Geosciences and Remote Sensing. 2011. 49 (12) 4815-4820.

Rizvi, I.A. and Buddhiraju, K.M., 2012: *Object-Based Analysis of Worldview-2 Imagery of Urban Areas.* IEEE International Geoscience and Remote Sensing Symposium, Munich, Germany.

Rizvi, I.A. and Buddharaju, K.M. *Improving the Accuracy of Object-Based Supervised Image Classification using Cloud Basis Functions Neural Network for High Resolution Satellite Images.* International Journal of Image Processing. 2010. 4 (4) 342-353.

Susaki, J. *Segmentation of Shadowed Buildings in Dense Urban Areas from Aerial Photographs.* IEEE Transaction on Geosciences and Remote Sensing. 2012. 4; 911-933.

Salvador, E., Cavallaro, A., and Ebrahimi, T. *Shadow Identification and Classification Using Invariant Color Models.* Proc. IEEE Int. Conf. Acoust., Speech, Signal Process. 2001. 3; 1545-1548.

Scott Papson and Narayanan Ram M. *Classification via the Shadow Region in SAR Imagery.* IEEE Transactions on Aerospace and Electronic Systems. 2012. 48 (2l).

Sarabandi, P., Yamazaki, F., Matsuoka, M. and Kiremidjian, K., 2004: *Shadow Detection and Radiometric Restoration in Satellite High Resolution Images.* In Proceedings of IEEE International Geoscience and Remote Sensing Symposium (IGARSS '04), Anchorage, AK, USA, 20-24 September 2004. 6; 3744-3747.

Song Huihui, Huang Bo and Zhang Kaihua. *Shadow Detection and Reconstruction in High Resolution Satellite Images via Morphological Filtering and Example-Based Learning.* IEEE Transaction on Geosciences and Remote Sensing. 2013. 52 (5) 2545-2554.

Tsai, V.J.D. *A Comparative Study on Shadow Compensation of Color Aerial Images in Invariant Color Models.* IEEE Transaction on Geosciences and Remote Sensing. 2006. 44 (6).

Wu Jindong, and Marvin E. Bauer. *Estimating Net Primary Production of Turf Grass in an Urban-Suburban Landscape with Quickbird Imagery.* Journal of Remote Sensing. 2012. 4; 849-866.

Yuan, F. *Land-Cover Change and Environmental Impact Analysis in the Greater Mankato Area of Minnesota using Remote Sensing and GIS Modeling.* International Journal of Remote Sensing. 2008. 29; 1169-1184.